

Application of Jatropha Oil in Heat Treatment of Aluminium Alloy 6061 and Corrosion Study of Anodized Alloy

Abubakar Garba Isah¹, Mohammed Salisu^{1,2}, Mohammed Umar Garba¹, Umaru Musa¹, Mohammed Alhassan, Mohammed Kutigi Idris²

¹Department of Chemical Engineering, Federal University of Technology, Minna, Niger State, Nigeria.

²Scientific Equipment Development Institute, Minna, Niger State, Nigeria.

Received 06 June 2021; Accepted 20 June 2021

Abstract: The application of Jatropha oil in heat treatment of aluminium alloy 6061 and corrosion behaviour of anodized alloy have been studied. The aim was to examine the effectiveness of Jatropha oil as alternative to mineral oil quenching media and also to examine the effectiveness of tartaric-sulphuric acid as alternative to chromic acid electrolyte for the anodization process. The aluminium alloy 6061 was prepared by melting high purity aluminium and other alloying elements at temperature 660 °C and cast into a cylindrical shape at 730 °C. The physicochemical properties (viscosity, acid value, iodine value and flash point) of Jatropha oil were evaluated. The aluminium alloy 6061 was heated to 530 °C for 2 hrs and quenched in Jatropha oil and mineral oil (SAE 20W/50) respectively and then age hardening at 120 °C for 5 hrs, anodization was conducted in a mixture of 80 g/l tartaric acid (C₄H₆O₆) and 40 g/l sulphuric acid (H₂SO₄) electrolyte under operating conditions of 13 V, period of 20 min and temperature of 37 °C. The results of these experiment shows that the composition (in wt. %) of alloy sample prepared was 95.93Al-1.1Mg-0.7Si, the physicochemical properties of Jatropha oil was characterized to be 162, 2.16 mg KOH/g sample, 13 gl/100g sample and 228 °C for the viscosity index, acid number, iodine value and flash point respectively. samples heat-treated to 530 °C and quenched in Jatropha oil has the highest tensile strength of 330 Mpa and yield strength of 284 Mpa. Increase solution treatment temperature was found in improved soluble precipitates in the alloy, and the heat extraction capacity of the quenching medium also contributed to the formation of fine precipitates. Improvements in properties may be correlated with a more refined metallurgical structure. High values of strength were associated with fine precipitate distribution.

I. INTRODUCTION

Aluminium alloy (AA 6061) is one of Al–Mg–Si (6xxx series) alloys were reported to have good corrosion resistances and optimum strength when subjected to solution heat treatment followed by quenching and tempering treatment (age-hardening) (Maisonnette *et al.*, 2011). The alloy is characterized to have better formability, weldability and lower density when compared with other aluminium alloys, hence resulted to their wide applications in the transport and the public domains (framework, pylon, handling equipment to mention but a few) and also for complex structures assembled by welding (Maisonnette *et al.*, 2011). Improving the strength of 6xxx series aluminium alloys by age-hardening is associated with the formation of magnesium silicate (Mg₂Si) precipitates. The presence of precipitates however, which are advantage to microstructural heterogeneity for strength development equally are setback to electrochemical heterogeneity for corrosion resistance (Kairy *et al.*, 2016). Thus, an increase in the alloy strength from precipitates is associated with increased susceptibility to localized corrosion such as pitting and intergranular corrosion (IGC) (Liang *et al.*, 2013).

The need to tackled the localized corrosion that do emanate amid heat treatment become necessary because the effect of unchecked corrosion therefore does not end up with the corroding utility itself but also covers the wide range of man and his economic and social welfare. The most commonly used corrosion control methods are materials selection and design, using corrosion-resistant alloys, protective coatings; use of special heat treatment; corrosion inhibitors. All of these methods are appropriate for controlling corrosion in certain situations and not for others. They are often used together to solve a particular corrosion problem (Madakson *et al.*, 2012). However, in order to improve their superficial mechanical properties, anodizing has been mostly used (Bensalah *et al.*, 2012).

Anodizing of Aluminium is a well-known electrochemical surface treatment during which an anodic oxide layer is formed on an Aluminium anode. Different electrolytes are commonly used, leading to the formation of a porous oxide with pore diameters and barrier layers membranes up to 200 µm thick. The electrolytes that can be used include chromic acid, sulfuric acid, oxalic acid, phosphoric acid, borates, citrate

and carbonates while employing either alternating or direct current (Sheasby, 2001; Alaaet al., 2013; Saeedikhani et al., 2013).

Chromic acid electrolyte is an effective way to produce oxide films with excellent resistant to corrosion during anodization. However, due toxicity of chromium it has since been prohibited. In order to find alternative to chromic acid electrolyte, several studies have been investigated using different acid electrolyte acids (Bensalah et al., 2012; Saeedikhani et al., 2013; Mubarok et al., 2015). Example of these acid electrolyte include boric-sulphuric acid (Thompson et al., 1999), sulphuric acid (Madakson et al., 2012), sulphuric-boric-phosphoric acids (Saeedikhani et al., 2012), sulphuric acid, oxalic acid, phosphoric acid (Abd-Elnaiem et al., 2013), phosphoric acid, sulphuric acid (Zuojia et al., 2014), sulphuric acid (Canepa et al., 2016) and sulphuric acid (Dumitrascu and Benea, 2017). Recently, the mixture of tartaric-sulphuric acid shows more promising results as an inhibitor and reduces dissolution of anodic oxide film and better corrosion protection performance. A number of works have been reported on the application of tartaric-sulphuric acid for anodization; Boisier et al. (2008) investigated the effect of tartaric acid on anodic film morphology and on corrosion resistance of hydrothermally sealed anodized AA 2024. It was observed that the properties of the barrier layer were higher when sealing was performed on specimens anodized in the presence of tartaric acid. This suggests a specific role of the species on the barrier layer, which contributes to the enhancement of the performance in terms of corrosion resistance of the sealed anodic films. On related report Mubarok et al. (2015) reported the influences of anodizing parameters of Al 2024 T3 in tartaric-sulphuric acid on the thickness, weight and corrosion resistance of the anodize layer. The authors demonstrated that the most influencing factor that determines the thickness and weight of the anodize layer is temperature, voltage and duration. The findings of the research reveal that pit density and current density were dependent on the coating thickness. Similarly, Fu et al. (2015) reported the effect of tartaric-sulphuric acid concentration on the anodic behaviour of titanium alloy, it was observed that 30 g/L tartaric acid addition to sulphuric acid increased the thickness of anodic film, decreased the crystallinity and weakened the dissolution rate of anodic film.

Based on the literatures reviewed so far sulfuric-tartaric acids electrolyte provided friendly environmental process and improved corrosion resistance; however the use of sulfuric/tartaric acid on the anodization of aluminium alloys (AA 6061) was poorly reported. This study proposed the use of electrolyte containing sulfuric-tartaric acids for the anodizing of 6061 aluminum alloy.

II. MATERIALS AND METHOD

The materials and equipment used during the experiments include 6061 Aluminum alloy. Quenching medium, melting furnace, heat treatment furnace, grinding machine, rotary wheel polishing machine, etching reagent, sulphuric-tartaric acid, hydrochloric acid, digital weighing machine, electrifier, and auxiliary wares for anodization set up.

2.1 Aluminium Alloy 6061 Development

For this study, the aluminium alloy (AA 6061) was prepared from aluminium cable wire (cut into smaller pieces) and weighed to 5 kg, magnesium metal powder and silicon carbide. Melting was conducted using charcoal-fire crucible. The molten metal was then poured into a cylindrical sand mould (350 mm length by 20 mm diameter) and allowed to cool. The cast alloy was then ejected from the mould and machined to sample size of 14 mm diameter and 10 mm length.

In order to determine the actual chemical composition of the cast AA 6061, an X-Ray Fluorescence (XRF) analysis was carried out on the cast specimen. The analytical result is shown in Table 1.

2.2 Determination of physicochemical properties of the oil

The oil under investigation (Jatropha oil) non-edible vegetable oil was obtained locally from Minna, Niger State, Nigeria. Investigation of physicochemical properties includes: Viscosity, acid value, iodine value and flash point.

Determination of Viscosity and Calculation of the Viscosity Index

The viscosity of jatropha oil was measured according to ASTM D445-06 (2011). The oil sample was placed into a glass U-tube. The sample was drawn through the tube using suction until it reached the starting position indicated on the tube side. The suction was then released, allowing the sample to flow back through the tube under gravity. The viscosity is reported in SI unit mm^2/s , equivalent to centistokes (cSt), and is calculated from the time it takes oil to flow from the starting point to the stopping point using a calibration constant supplied for each tube. An average of independent five measurement of viscosity test at temperatures of 40 °C and 100 °C.

viscosity index is an arbitrary number indicating the effect of change of temperature on the kinematic viscosity of oil. A high viscosity index signifies relatively small change of kinematic viscosity with temperature. The viscosity index oil was calculated from its viscosities at 40 and 100 °C. The procedure for the calculation is given in ASTM Method D 2270-74 for calculating viscosity index from kinematic viscosity at 40 and 100 °C.

$$\text{Viscosity Index (VI)} = \left(\frac{L-U}{L-H} \right) * 100 \quad (1)$$

where:

L = kinematic viscosity at 40 °C of an oil of 0 viscosity index having the same kinematic viscosity at 100 °C as the oil whose viscosity index is to be calculated, mm²/s (cSt),

H = kinematic viscosity at 40 °C of an oil of 100 viscosity index having the same kinematic viscosity at 100 °C as the oil whose viscosity index is to be calculated mm²/s (cSt).

U = kinematic viscosity at 40 °C of the oil whose viscosity index is to be calculated mm²/s (cSt).

Determination of Acid Number

As oil degrades, it forms acidic by-products. Chemical analysis can identify and measure these by-products. The acid number (AN) is the most common method employed. The AN was determined by a titration procedure using potassium hydroxide (KOH) and was reported as milligrams of KOH per gram of sample (mg KOH/g). AN is given by the expression (Canaleet al, 2005):

$$\text{AN} = \frac{56.1 * \text{NV}}{W} \left[\text{mg} \frac{\text{KOH}}{\text{g}} \right] \quad (2)$$

Where;

56.1 = molar mass of the KOH

V = Volume of KOH solution in ml

N = Normality of KOH solution

W = Weight of sample in g

Determination of Iodine Value

The iodine value is a measure of the degree of unsaturation in oil and could be used to quantify the amount of double bonds present in the oil which reflects the susceptibility of oil to oxidation. Iodine number was determined according to ASTM D5554-95. 0.4 g of the sample was weighed into a conical flask and 20 cm³ of carbon tetrachloride was added to dissolve the oil. Then 25 cm³ of Dam's reagent was added to the flask using a safety pipette in fume chamber. Stopper was then inserted and the content of the flask was vigorously swirled. The flask was then placed in the dark for 2 hours 30 minutes. At the end of this period, 20 cm³ of 10% aqueous potassium iodide and 125 cm³ of water were added using a measuring cylinder. The content was titrated with 0.1 M sodium thiosulphate solutions until the yellow colour almost disappeared.

Few drops of 1% starch indicator was added and the titration continued by adding thiosulphate drop wise until blue coloration disappeared after vigorous shaking. The same procedure was used for blank test and other samples. The iodine value (I.V) is given according to ASTM D5554-95:

$$\text{I.V} = \frac{12.69C(V_1 - V_2)}{M} \quad (3)$$

Where;

C= Concentration of sodium

V₁= Volume of sodium thiosulphate (Na₂S₂O₃) solution used to titrate the blank,

V₂ = Volume of sodium thiosulphate solution used to titrate the sample.

M = Mass of the sample

2.3 Tensile Properties Test

The tensile properties of the quenched steel sample were carried out using "MONSO TENSOMETER" After measuring initial gauge length (l₀) and diameter, the specimen testing was done, the graphs of load versus extension were plotted on a graph paper fixed to the stylus from which yield load, maximum load, were taken for the calculation of yield strength and tensile strength respectively.

2.4 Anodization Process

Before the anodizing operation the surface of the samples were pre-treated with solution of 0.5 M NaOH for 5 min at 45°C and desmutting in 5 vol.% HNO₃ for 5 min at 25°C (Talib and Khalid, 2015); anodization operation was carried out in a mixed electrolyte of sulfuric-tartaric acid (40 g/l H₂SO₄ + 80 g/l C₄H₆O₆) at a voltage of 12-13 V, period of 20 min and temperature 37°C (Capelossiet al., 2015). After each steps, the specimens were neutralized by rinsing in distilled water to avoid contamination of solution of the subsequent operations. The details for the procedure can be found in (Saeedikhani et al., 2013).

2.5 Corrosion Test

Prepared coupon samples are subjected to both weight loss and linear polarization resistance corrosion studies in 3.5 wt% NaCl solution.

2.5.1 Weight Loss Corrosion Coupon Analysis.

All test coupons were cleaned, weighed and stored in a desiccator. The weighed coupons completely immersed in 250 ml bowl containing the corrosive media (3.5 wt% NaCl). Weight losses of coupons were taken at interval of 72 hrs (3 days) over a period of 504 hrs (21 days). Prior to weight measurement of each coupon, the surface was scrubbed with brush in distilled water and then rinse in ethanol in order to remove corrosion product and then air dried. The weight loss was calculated by taken the differences between the weight before immersion and the weight after immersion. Each weight was measured to the nearest 0.01 g on a laboratory weighing balance.

Calculation of the corrosion rate will be in mm/year, by applying the formula;

$$\text{CPR} = \frac{87.6\Delta W}{\text{DAT}} \left(\frac{\text{mm}}{\text{yr}} \right) \quad (1)$$

Where;

ΔW = weight loss in mg = $W_o - W_f$

W_o = original weight of the coupons

W_f = final weight of the coupons after 3 days

D = density of aluminium alloy in g/cm^3 = mass/volume of substance

A = total surface area of the samples in cm^2

T = exposure time in hours, in the corrosive medium (Madakson *et al.*, 2012).

2.5.2 Potentiodynamic Polarization Analysis

The electrochemical corrosion behaviours was characterized by potentiodynamic polarization, it was conducted by applying current density 40 A/cm² and a scan rate of 0.001 V/s from potential of -1,500 to +1,500 by a PGSTAT 204 electrochemical analyzer (Netherlands) in 3.5 wt% NaCl solution at room

temperature. The corrosion parameters evaluated includes; corrosion potential (E_{corr}), Corrosion current (I_{corr}) for the AA 6061 specimens. Before testing, the specimens were immersed in NaCl solution for about 30 min in order to stabilize the open circuit potential. In the process the potentiostat was coupled to a computer, a glass corrosion kit with graphite rods as counter electrode and a saturated Ag/Ag 3 M KCl electrode was also used as the reference electrode. The specimens (working electrodes) was tightly mounted and positioned at the glass corrosion cell kit leaving the average of 0.8262 cm² surfaces in contact with the electrolyte. Polarization curves were plotted using excel Microsoft application, both the corrosion rate and potential were then estimate for the anodic and cathodic branches of polarization curves in accordance to the method of (Shen *et al.*, 2015; Abdullahi, 2016).

2.6 Surface morphology studies

Scanning Electron Microscopy (SEM)/ Energy Dispersive Spectroscopy (EDS)

Scanning electron microscopy (SEM) was performed on an Amary 1910 field emission SEM at 20 kV in a high vacuum environment and X-ray energy dispersive spectroscopy (EDS) spectra was collected and analyzed using Link ISIS system.

III. RESULTS AND DISCUSSION

The results obtained after successfully conducting the experiments are as follows:

3.1 Chemical composition analysis of the cast AA 6061

The result of the X-ray fluorescence (XRF) analysis was carried out using EDXRF Model: Minpal 4 No. DY 1055 manufactured by PANalytical B.V and the result is presented in Table 1.

Aluminium alloy (AA 6061) is one of Al–Mg–Si (6000 series) (Kairyet *et al.*, 2015). The composition (in wt. %) obtained for the as-cast AA 6061 as shown in Table 4.1 was 95.93Al-1.1Mg-0.7Si. This value falls within the range of Yu *et al.*, (2002) who reported 96.20Al- 0.8-1.2Mg-0.15Si and also with the value of ASTM B247 as 95.7999-98.6099Al- 0.8-1.2Mg-0.4-0.8Si but with slight difference from Dumitracus and Benea (2017) who reported 97.86Al-0.8Mg-0.4Si. However, in contrast with Abubakreet *et al.*, (2009) who reported 89.6875Al-2.1515Mg-4.4174Si. The inconsistency in the result could be attributed to the raw material and operating condition of casting.

Table 1: Chemical Composition (wt. %) of Prepared AA 6061 Sample

Element	% Composition				
	This work	1	2	3	ASTM
Al	95.93	97.4-96.35	98.05	89.68	95.80 – 98.61
Si	0.7	0.15	0.4	4.42	0.4 – 0.8
Fe	0.5	0.4-0.8	0.2	0.63	0.0 – 0.7
Cu	0.35	0.15-0.4	0.15	0.14	0.15 – 0.4
Mn	0.15	0.7	0.15	2.06	0.0 – 0.15
Mg	1.1	0.8-1.2	0.8	2.52	0.8 – 1.2
Cr	0.9	-	-	0.02	0.04 – 0.35
Zn	0.25	0.25	0.25	0.65	0.0 – 0.25
Ti	0.12	0.15	-	0.01	0.0 – 0.15

Source: ¹Dumitracus and Benea, 2017, ²Yu *et al.*, 2002 and ³Abubakre *et al.*, 2009

3.2 Physicochemical properties of jatropha oil

The results of physicochemical properties of jatropha oil which include; viscosity index, acid number, iodine value and flash point are presented in Table 2.

The rate at which the viscosity of oil will change as the temperature changes is called viscosity index. The viscosity index of the Jatropha oil was determined according to ASTM D2270. For this study the viscosity index (VI) value of the Jatropha oil was reasonable high to about 162. This implies that the viscosity of the oil would not change much with temperature variation and this is in agreement with the report of Agboola *et al* (2015).

The acid value of 2.16 mg KOH/g sample was considered to be low and fall within the acceptable limit. According Canale *et al.*, (2005) the recommended value for quenching oil is between 0.00 to 3.00 mg KOH/g sample.

Iodine value is a measure of the unsaturations content or double bonds present in the oil which shows the proneness of oil to oxidation. The iodine value of Jatropha oil analyzed is 13 gl/100 g samples which indicated low percentage of unsaturated fatty acids in the oil.

The flash point of the Jatropha oil was recorded high having value of 228 °C. This shows that the vapour blanket stage could be longer, indicating low fire risk as the quantity of volatile constituents are minimal or none. This value is in agreement with standard values (190-210 °C) reported for standard oils (Agboola *et al.*, 2015).

Table 2: Summary of physicochemical properties of Jatropha oil

	Viscosity at 40 °C (mm ² /s)	Viscosity at 100 °C (mm ² /s)	Viscosity Index	Acid number (mg KOH/g sample)	Iodine value (gl/100g sample)	Flash point (°C)
Jatropha oil	33.5	7.44	162	2.16	13	228

3.3 Tensile strength and microstructure of aluminium alloy 6061

Tensile strength

The results of the tensile strength test are shown in Table 3 when the samples are heated to 530 °C. The highest ultimate tensile strength values were obtained in samples quenched in Jatropha oil has the highest ultimate strength of 330 Mpa follow by SAE 20W/50 engine oil with 305Mpa. Similarly the yield strength obtained was 284 Mpa and 292 Mpa respectively. The values for the as-cast are ultimate tensile strength 275 Mpa and yield strength of 237 Mpa. Samples quenched in Jatropha oil at 530 °C showed a marginal increase in strengths (ultimate and yield strength) when compared to the values for the as-cast sample. According to Dauda *et al.*, (2015) the values of tensile strength are influenced by the microstructure of the aluminum alloy sample, which are controlled by the quenchant's cooling rate. This show that the high strength produced is due to the effectiveness of the quenchants.

Table 3: Tensile Test result of AA 6061 samples

Media	Ultimate strength Mpa	Yield Strength Mpa	% Elongation
Jatropha oil	330	284	18
Engine oil	305	292	16
As-cast	275	237	14

3.4 Microstructure of AA 6061

The microstructure of the as-cast and heat treated samples were viewed under metallurgical microscope and are presented in Figure 1A – 1C

The black and white portion observed indicated the presence of Mg_2Si and $\alpha-Al$ respectively as shown in Figure 1A. The phases observed are in agreement with the Al-Mg-Si phase diagram Georgatset *al.*, (2012).

Figure 1B and Figure 1C shows the microstructure of Jatropha oil and engine oil quenched respectively, fine precipitates which are uniformly distributed in the Aluminium matrix was observed which could be responsible for the improvement in the values of ultimate tensile strength as shown in Table 3, as compared to as-cast which have precipitate that are coarsely distributed. The microstructural changes in the quenched samples are associated with the temperature of solutioning and the cooling rate. This is in agreement with Abubakaret *al.*, (2009), who reported that hardness and strength increases as grain size decreases. More spherodised grains is observed in the structure samples quenched in Jatropha oil, this is in agreement with report of Zainonet *al.*, (2015) who reported that precipitates of this phase do not only affect mechanical properties the strength is also influenced by the intermetallic phases formed during solidification of the alloys.

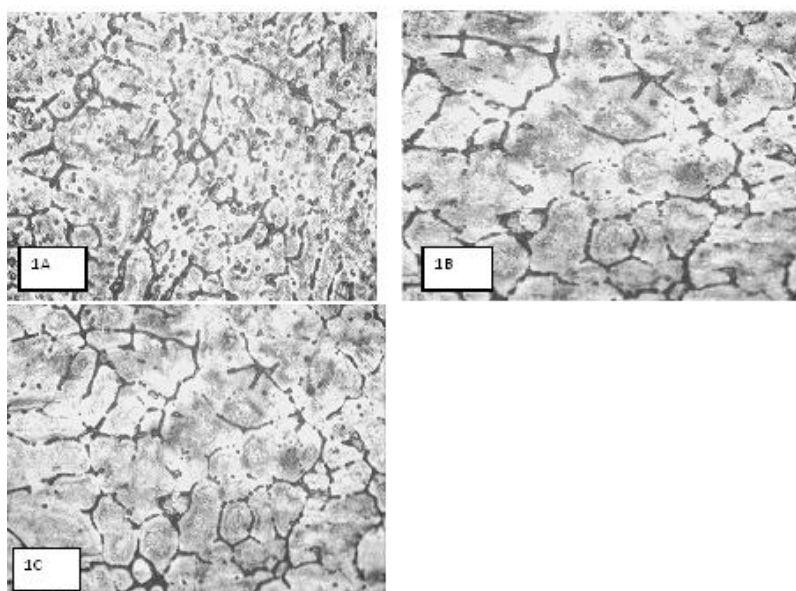


Figure 1: Microstructure of AA 6061 of as cast (A), Jatropha oil quenched (B), and SAE 20/50W engine oil quenched (C) in 100X

3.5 Effect of heat treatment and anodization on the corrosion resistance of AA 6061

Weight Loss Corrosion Coupon Test

The results of the corrosion behaviour of unanodized and anodized samples obtained by weight loss coupon test were presented in Figure 2A – 2D.

The results of corrosion penetration rate (CPR) of unanodized and anodized AA 6061 coupons exposed to sodium chloride (3.5 wt. % NaCl) solution at interval 72 hrs (3 days) over a period of 504 hrs (21 days). The corrosion penetration as a function of time is shown in Figures 4.2-4.5. Figure 2A shows that the corrosion rate attained the highest point of 0.060 mm/yr for sample quenched in Jatropha oil before it begin to declined, follow by sample quenched in SAE 20W/50 which attained the highest point of 0.048 mm/yr then finally as cast recorded the least point of 0.038 mm/yr before decline. This variation may be attributed to the quenching effect in different media.

From Figure 2B–2D, there was initial increase in corrosion rate for both anodized and unanodized coupons then followed a decrease with exposure time. This result demonstrated the normal corrosion rate profile of

passivating metals when subjected to corrosive environments. The nature firstly rise in the corrosion rate going with the active region until it attained the highest point leading to formation of oxide on the samples metal the corrosion rate decreases due to passivity. At certain stage there was fluctuation of increase then decrease this could be as result of trans-passivity region. In comparison the unanodized coupon samples corrode faster than the anodized.

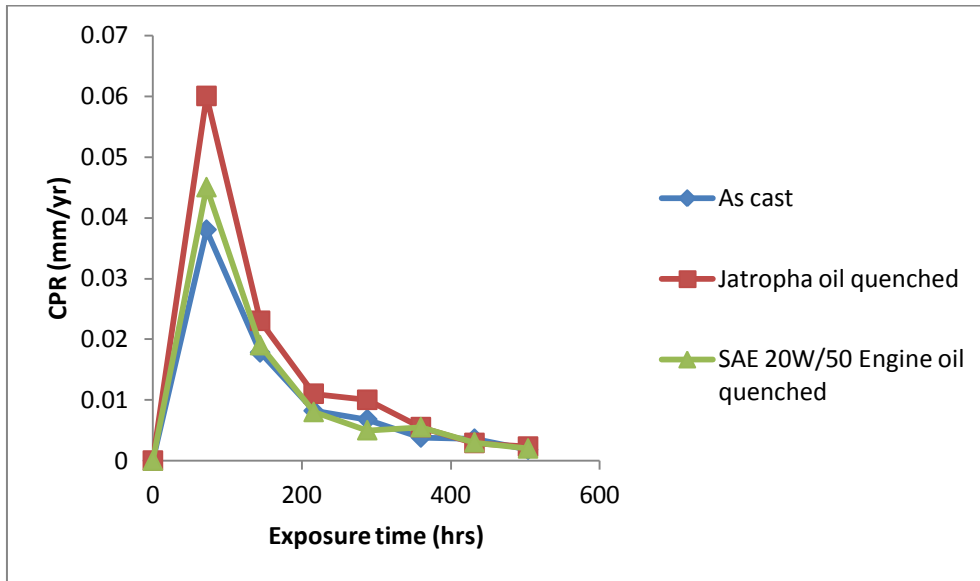


Figure2A: Corrosion Rate of Unanodized Al alloy 6061 As-cast, Jatropha oil quenched, and SAE 20W/50 Engine oil quenched samples Against Exposure Time in 3.5 wt. % NaCl solution

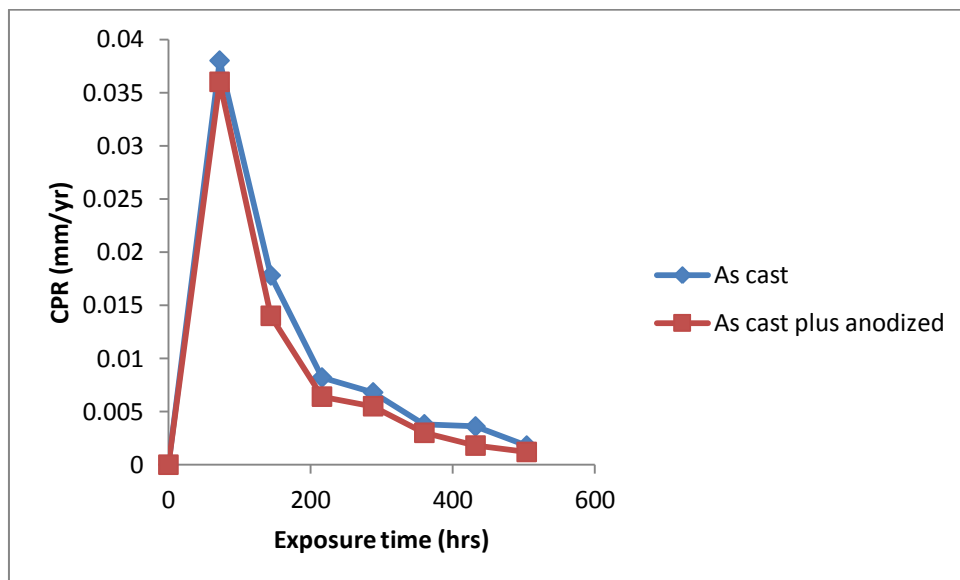


Figure2B: Corrosion Rate of Unanodized and Anodized Al alloy 6061 As-cast samples Against Exposure Time in 0.5 M NaCl solution

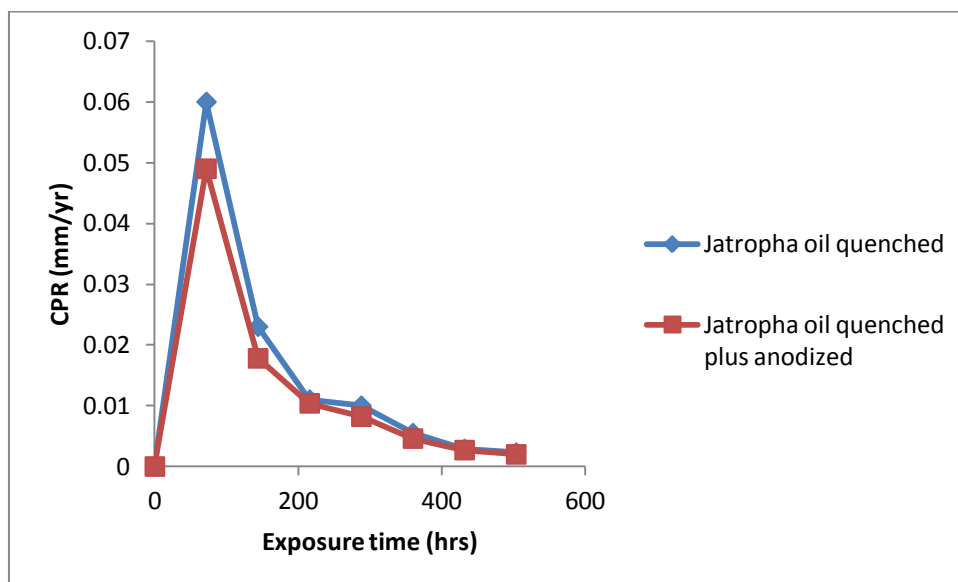


Figure2C: Corrosion Rate of Unanodized and Anodized Al alloy 6061 As-cast, Jatropha oil quenched samples Against Exposure Time in 3.5 wt. % NaCl solution.

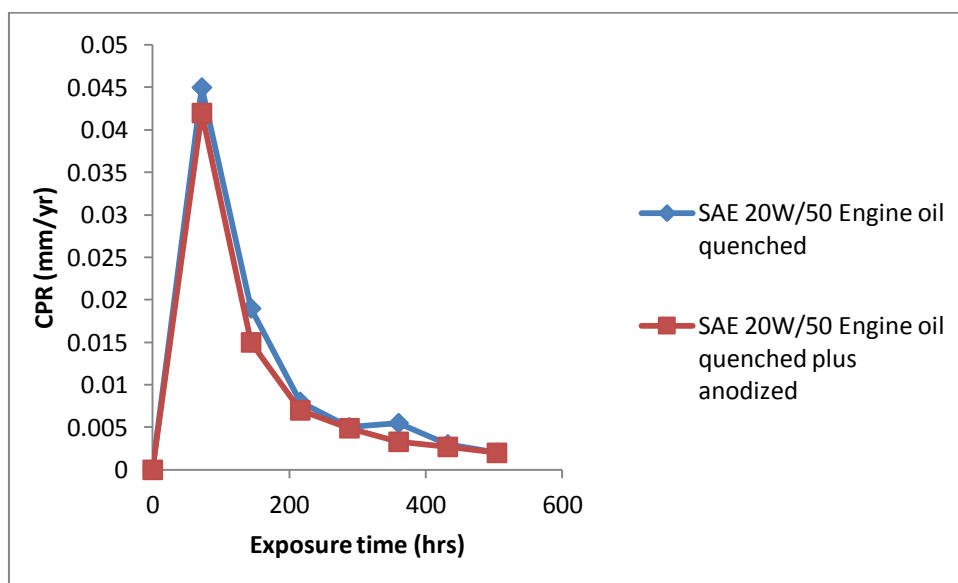


Figure2D: Corrosion Rate of Unanodized and Anodized Al alloy 6061 SAE 20W/50 Engine oil quenched samples Against Exposure Time in 3.5 wt. % NaCl solution.

Potentiodynamic Polarization Analysis

The electrochemical corrosion behaviours were characterized by potentiodynamic polarization using PGSTAT 204 electrochemical analyzer (Netherlands).

The as-cast, heat treated and anodized samples as compared to the unanodized samples, measured in 3.5 wt % NaCl solution after immersion for 1 h. The corrosion potential (E_{corr}) and the corrosion current density (I_{corr}) for each specimen were estimated, summarized in Table 4. E_{corr} was shifted slightly to be more positive for anodized as-cast (-1.234 V), Jatropha oil quenched (-1.5024 V), and engine oil quenched (-1.3197 V) samples, compared to unanodized as-cast (-1.2389 V), Jatropha oil quenched (-1.7196 V), and engine oil quenched (-1.6306 V) samples. Meanwhile, I_{corr} decreased significantly for unanodized as-cast (2.75×10^{-6} A/cm²), Jatropha oil quenched (1.27×10^{-6} A/cm²), and engine oil quenched (3.96×10^{-6} A/cm²) samples compared to anodized as-cast (1.69×10^{-6} A/cm²), Jatropha oil quenched (1.14×10^{-6} A/cm²), and engine oil quenched (2.94×10^{-6} A/cm²). The I_{corr} variation between the anodized and unanodized could be due to passivating oxide layer formed on the anodized. In relating the result with the work of Jeong *et al.*, (2015), this indicates an improvement in the corrosion protection properties of the surfaces in that order.

Table 4: Potentiodynamic polarization parameters of as cast, heat treated and anodized AA6061 samples exposed to 3.5 wt.% NaCl.

Samples	I _{corr} (A/cm ²)	E _{corr} (V)	Polarization resistance (Ω)	Corrosion rate (mm/year)
As-cast (1)	2.75E-06	-1.234	7304.4	0.031935
Jatropha oil quenched (2)	1.27E-06	-1.5024	2406	0.05197
Engine oil quenched (3)	2.94E-06	-1.3197	6926.3	0.046025
As-cast plus anodized (A1)	1.69E-06	-1.2389	14744	0.019626
J/oil quenched plus anodized (A2)	1.14E-06	-1.7196	1526.1	0.019293
E/oil plus anodized (A3)	1.14E-06	-1.6306	1226.9	0.012693

3.6 Surface examinations

Scanning Electron Microscope (SEM) Observations.

The morphology of the unanodized and anodic layers was investigated using Model No. EVO MA-10 SEM manufacture by Carl. The observations were presented in Figures 3.1-3.3.

Both unanodized and anodized specimens were analyzed by Scanning Electron Microscope (SEM) in order to study the surface layer and the growth of anodized coatings. Figure 3.1- 3.3 shows the SEM of unanodized and anodized aluminium alloy 6061 obtained from sulfuric-tartaric acid.

Figure 3.1A, 3.1A and 3.3A shows the plane surface layer of unanodized as-cast, jatropha oil quenched and SAE W20/50 engine oil quenched respectively. The surfaces does not reveal coating layer except few whitish spot which could be associated with heterogeneous distribution of the alloying element.

The cross-section morphology of anodic film of the AA 6061 is shown in Figure 3.1B, 3.2B and 3.3B, respectively. The porous layer and barrier layer cannot be clearly distinguished in the SEM images, but the oxide film thickness could be observed.

Figure 3.1C, 3.2C and 3.3C shows compact layer with less surface pores on the top view. The compact layer could be attributed to low operating temperature and slower oxide layer dissolution rate. This observation was in agreement with the report of Mubaroket *al.*, 2015 who reported that at temperature below 40 °C, dissolution of oxide film takes place slower than that at higher temperatures. Other author Saeedikhani *et al.*, 2013 reported that sealing consists of a general reduction of sectional area of each pore with the formation of a “plug” in the pore bottom.

The porous structure of the covering layer obtained in the presence of tartrate seemed to be comparable to that reported by Bensalahet *al.*, (2012) for the case of conversion coatings formed on aluminum treated in chromate- phosphate containing solutions.

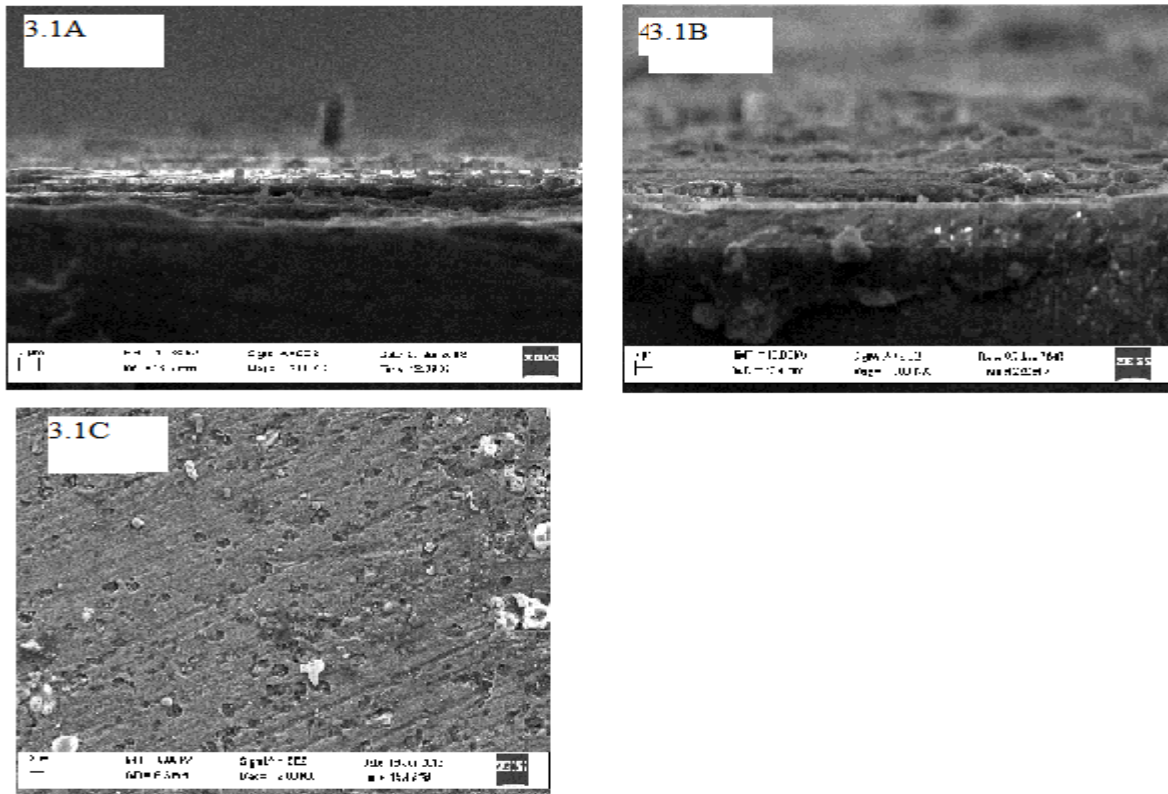


Figure 3.1: SEM micrographs of as-cast AA 6061 (A) cross section of the unanodized (B) cross section of the oxide coating formed by anodization (C) top view of the oxide coating formed by anodization.

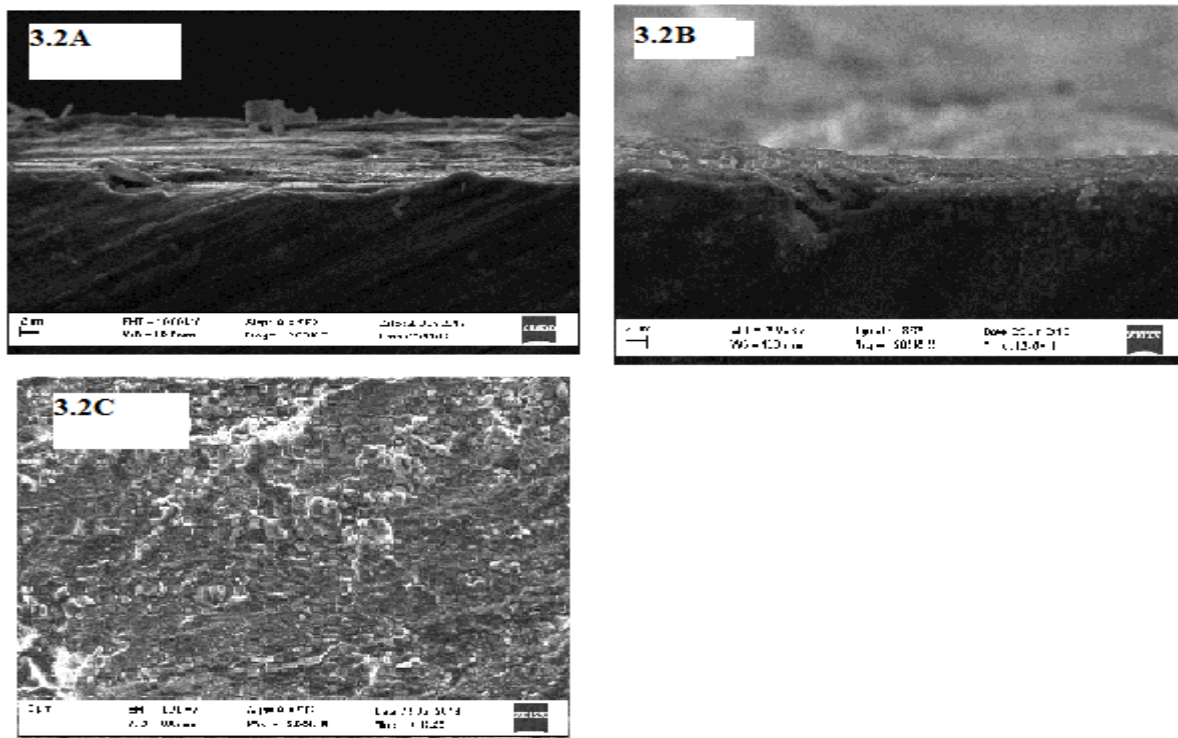


Figure 3.2: SEM micrographs of Jatropha oil quenched AA 6061 (A) cross section of the unanodized (B) cross section of the oxide coating formed by anodization (C) top view of the oxide coating formed by anodization.

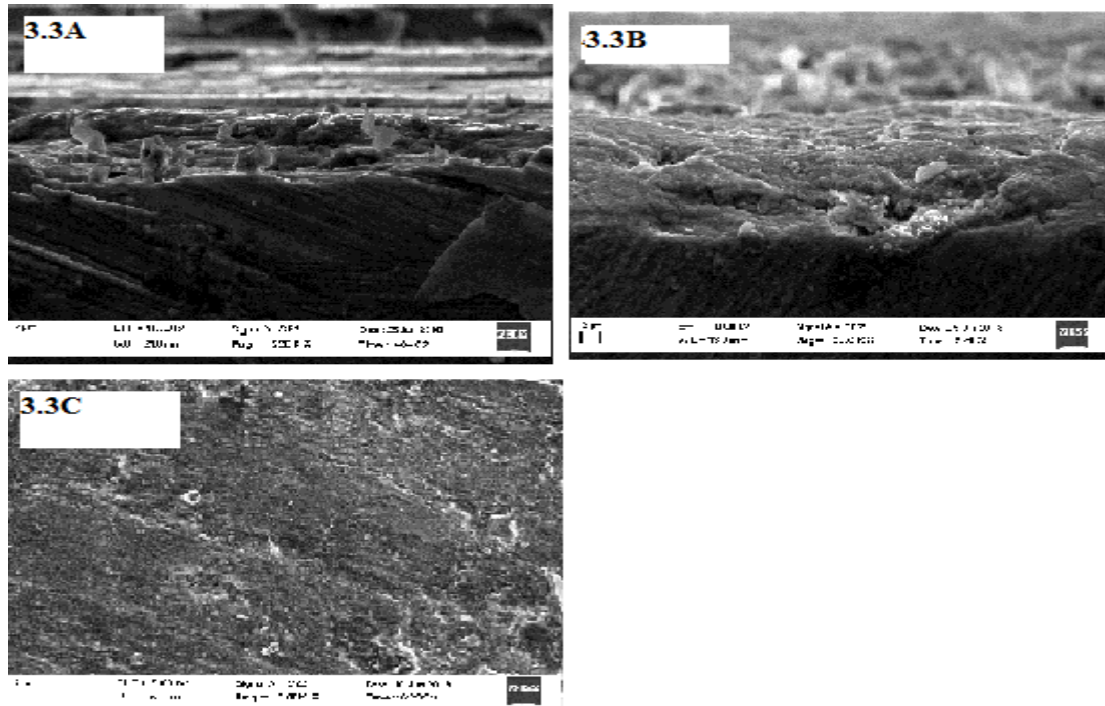


Figure 3.3: SEM micrographs of SAE 20/50W engine oil quenched AA 6061 (A) cross section of the unanodized (B) cross section of the oxide coating formed by anodization (C) top view of the oxide coating formed by anodization.

IV. CONCLUSIONS:

The following conclusions can be drawn from the research.

- i. Characterization of the produced aluminium alloy sample was done with X-ray fluorescence (XRF), the chemical composition of Mg and Si being the main alloying elements for AA 6061 falls within the acceptable range of 0.8-1.2 for Mg and 0.4-0.8 for Si respectively.
- ii. The physicochemical properties that have direct influence on the quenching were evaluated and the report shows that the Jatropha oils are suitable as potential quenching media for AA 6061.
- iii. The microstructure of the as-cast and heat treated samples has been studied under metallurgical microscope. Increase solution treatment temperature was found to improve soluble precipitates in the alloy, and the heat extraction capacity of the quenching medium also contributed to the formation of fine precipitates. Improvements in properties may be correlated with a more refined metallurgical structure. High values of strength were associated with fine precipitate distribution.
- iv. The effect of sulphuric-tartaric acid anodization on the corrosion behaviour of heat treated AA 6061 has been studied in sodium chloride. As a result of this investigation, it was revealed that both as-cast and heat treated aluminium alloy 6061 corroded in sodium chloride solution with the heat treated sample being the fastest. Anodization with sulphuric-tartaric acid electrolyte reduced the corrosion rate of aluminium alloy 6061 in sodium chloride solution. In correlation with the linear polarization techniques similar trend of corrosion inhibition due to anodization was established. It was concluded that sulphuric-tartaric acid can be used as electrolyte to improve the corrosion resistance of aluminium alloy 6061.
- v. The morphology of the unanodized and anodic layers was investigated. The SEM micrographs show the pore character of the oxide layer. Energy Dispersive Spectroscopy (EDS) spectra were collected along with the SEM. The elemental composition corroborates microstructural analysis results; species of tartrate and sulphur were observed on the anodized samples.

ACKNOWLEDGMENT

The authors wish to thank both the managements and staffs of Scientific Equipment Development Institute, Minna and Federal University of Technology, Minna for making this research work a success.

REFERENCES

- [1]. Abdullahi, M. (2016). Investigation of the Effect of Heat Treatment and Anodization on the of Aluminium Alloy (AA 7075). MSc unpublished Thesis, Faculty of Engineering, Ahmadu Bello University, Zaria, Nigeria.

- [2]. Abubakre, O.K., Mamaki, U. P., & Muriana, R. A. (2009). Investigation of the Quenching Properties of Selected Media on 6061 Aluminum Alloy. *Journal of Minerals & Materials Characterization & Engineering*, 8(4), 303-315.
- [3]. Agboola, J.B., Abubakre, O.K., Mudiare, E., Adeyemi M.B., & Hassan, S.B. (2015). Physico-chemical Characteristics and Fatty Acids Composition of Some Selected Nigerian Vegetable Oils for Quenching Medium. *British Journal of Applied Science & Technology*, 8(3), 246-253.
- [4]. Alaa, M., AbdElnaiem, A., Mebed, A.M., Gaber, A., & Abdel-Rahim, M.A. (2013). Effect of the Anodization Parameters on the Volume Expansion of Anodized Aluminum Films, *International Journal Electrochem. Sci.*, 8, 10515 – 10525.
- [5]. American Society of Testing and Materials (2009). Standard Test Method for Iodine number. New York. American Society of Testing and Materials, 16:45-50.
- [6]. Boisier, G., Pébère, N., Druetz, C., Villatte, M. and Suel, S. (2008) FESEM and EIS Study of Sealed AA2024 T3 Anodized in Sulfuric
- [7]. Acid Electrolytes: Influence of Tartaric Acid. *Journal of the Electrochemical Society (JES)*, **155**, 521-529
- [8]. Bensalah, W., Elleuch, K., Feki, M., Depetris-Wery, M., & Ayedi, H.F (2012). Optimization of tartaric/sulphuric acid anodizing process using Doehlert design. *Surface & Coatings Technology*, 207, 123–129.
- [9]. Canale, L.C.F., Fernandes, M.R., Augustinho, S.C.M., Totten, G.E., & Farah, A.F. (2005). Oxidation of vegetable oils and its impact on quenching performance, *International Journal of Materials and Product Technology*. 24(1-4):101-125.
- [10]. Capelossi, V.R., Poelman, M., Hernandez, R.P.B., Melo, H.G.D. and Olivier, M.G. (2014). Corrosion Protection of Clad 2024 Aluminum Alloy Anodized in Tartaric-Sulfuric Acid Bath and Protected with Hybrid Sol-Gel Coating. *Electrochimica Acta*, 124, 60-79
- [11]. Dauda, M., L. Kuburi, S., Obada, D.O., & R. I. Mustapha, R.I. (2015). Effects of Various Quenching Media on Mechanical Properties of Annealed 0.509wt% C –0.178wt% Mn Steel. *Nigerian Journal of Technology (NIJOTECH)*, 34(3), 506 – 512.
- [12]. Dumitrascu, V. M., Benea, L. (2017). Improving the Corrosion Behaviour of 6061 Aluminum Alloy by Controlled Anodic Formed Oxide Layer. *REV.CHIM. (Bucharest)*, 68(1).
- [13]. Fu C., Hongxing L., Mei Y., Jianhua L., Songmei L.. (2015). Effect of Tartaric Acid Concentration on the Anodic Behaviour of Titanium Alloy, *Int. J. Electrochem. Sci.*, 10, 4241 – 4251.
- [14]. Georgatis, A., Lekatou, A. Karantzalis, E., Petropoulos, H., Katsamakias S., & Poulia, A. (2012). Development of a Cast Al-Mg₂Si-Si In Situ Composite: Microstructure, Heat Treatment, and Mechanical Properties. *Journal of Material Engineering Performance*, 22, (3), 729–741.
- [15]. Jeong, C., Junghoon, L., Keith, S., & Chang-Hwan C. (2015). Air-Impregnated Nanoporous Anodic Aluminum Oxide Layers for Enhancing the Corrosion Resistance of Aluminum. American Chemistry Society Publication.
- [16]. Kairy, S.K., Rometscha, P.A., Diaob, K., Niew, J.F., Davies, C.H.J., & Birbilisa, N. (2016). Cu Exploring the electrochemistry of 6xxx series aluminium alloys as a function of Si to Mg ratio, content, ageing conditions and microstructure. *Electrochimica Acta*, 190, 92–103.
- [17]. Liang, W.J., Rometsch, P.A., Cao, L.F., Birbilis, N. (2013). General aspects related to the corrosion of 6xxx series aluminium alloys: Exploring the influence of Mg/Si ratio and Cu Corrosion Science, 76, 119–128.
- [18]. Li, F., Zhang, L., & Metzger, R. (1998). On the growth of highly ordered pores in anodized aluminium oxide, *Chemistry of Materials*. American Chemical Society Publication. 10(9), 2470-2480.
- [19]. Madakson, P. B., Malik, I. A., Laminu, S. K., & Bashir, I. G. (2012). Effect of Anodization on the corrosion behavior of Aluminium Alloy in HCl acid and NaOH. *International Journal Materials Engineering*, 2(4), 38-42.
- [20]. Maissonnette, D., Suery M., Nelias D., Chaudet, P., & Epicier, T. (2011). Effects of Heat Treatments on the Microstructure and Mechanical Properties of a 6061 Aluminium Alloy. *Materials Science and Engineering A*, 528, 2718–2724.
- [21]. Mubarak M. Z., Wahab S. & Soleh W. (2015). Effects of Anodizing Parameters in Sulphuric-Tartaric acid on Coating Thickness and Corrosion Resistance of Al 2024 T3 Alloy. *Journal of Minerals and Materials Characterization and Engineering*, 3, 154-163
- [22]. Saeedikhani, M., Javidi, M., & A. Yazdani, A. (2013). Anodizing of 2024-T3 aluminum alloy in, sulfuric–boric–phosphoric acids and its corrosion behaviour, *Transition, Nonferrous Metal Society, China*, 23, 2551–2559.
- [23]. Sheasby P.G., Wernick S., & Pinner R. (2001). *The Surface Treatment and Finishing of Aluminium and its Alloys 2* (sixth edition), UK: ASM international and finishing publications.

- [24]. Shen, Y.Z., Li H.G., Tao H.J., Ling J., Wang, T. & Tao J. (2015). Effect of Anodic Films on Corrosion Resistance and Fatigue Crack Initiator of 2060-T8 Al-Li Alloy. *International Journal Electrochemistry Science*, 10, 938 – 946
- [25]. Talib, M.N., & Khalid H.R., Comparative Study for Anodizing Aluminium Alloy 1060 by Different Types of Electrolytes Solutions. Retrieved from <http://.uotechnology.edu.iq/dep-chem-eng/PAPERS/taleb%20kaled%20h%20x.pdf>.
- [26]. Thompson G. E, Zhang L, Smith C. J. E, Skeldon P. (1999). Boric/sulphuric acid anodizing of aluminum alloys 2024 and 7075: Film growth and corrosion resistance [J]. *Corrosion Science*, 55(11), 1052–1061
- [27]. Yu, X., Chuanwei, Y., Chunan C., (2002). Study on the rare earth sealing procedure of the porous film of anodized Al6061/SiCp. *Materials Chemistry and Physics*, 76, 228–235.
- [28]. Zainon, F., Khairrel, R. A., & Ruslizam D., (2015). Effect of Heat Treatment on Microstructure, Hardness and Wear of Aluminum Alloy 332. *Applied Mechanics and Materials*, 786, 18-22.
- [29]. Zuoja, L.I., Xiaohui, L., Donatus, U., George. E. T., and Peter. S.k., (2014). Corrosion Behaviour of the Anodic Oxide Film on Commercially Pure Titanium in NaCl Environment. *International Journal Electrochemistry Science*, 9, 3558 – 3573.

Abubakar Garba Isah, et. al. “Application of Jatropha Oil in Heat Treatment of Aluminium Alloy 6061 and Corrosion Study of Anodized Alloy.” *IOSR Journal of Engineering (IOSRJEN)*, 11(06), 2021, pp. 15-27.